



A term structure interest rate model with the Brownian bridge lower bound

Kentaro Kikuchi¹

Received: 31 March 2023 / Accepted: 21 February 2024

© The Author(s), under exclusive licence to Springer-Verlag GmbH Germany, part of Springer Nature 2024

Abstract

We present a new quadratic Gaussian short rate model with a stochastic lower bound to capture changes in the yield curve including negative interest rates, associated with changes in monetary policy stances. We model the lower bound by a Brownian bridge pinned at zero at the initial time and at a random termination time, representing the first appearance of negative interest rates and the end date of an unconventional monetary policy, respectively. Within this framework, we derive a semi-analytical pricing formula for zero coupon bonds under the no-arbitrage condition. Our model estimation results using Japanese yield curve data show a good fit to the market data. Furthermore, the expected excess bond returns and the posterior distribution of the unconventional monetary policy duration computed from the model parameter and state variable estimates clarify the market's perspective on monetary policy developments.

Keywords No-arbitrage condition · Quadratic Gaussian term structure model · Brownian bridge · Negative interest rate · Unconventional monetary policy

JEL Classification E43 · E52 · G12

1 Introduction

A term structure interest rate model is often used to extract market expectations of future interest rate movements from a time series of yield curve observations. To achieve this, such a model should fit the market yield curves at each point in time and capture the probability distribution of future interest rate levels.

The affine Gaussian term structure model (ATSM) is one such tool, and is widely used for analyzing the time series of yield curves, primarily owing to its analytical simplicity and ease of estimation. For example, the studies by Ang and Piazzesi (2003)

✉ Kentaro Kikuchi
kentaro-kikuchi@biwako.shiga-u.ac.jp

¹ Faculty of Economics, Shiga University, Banba, Hikone, Shiga 522-8522, Japan

and Kim and Orphanides (2012) apply the ATSM to extract market expectations from US Treasury yield data. A common assumption in many empirical analyses using the ATSM, including the aforementioned studies, is that the state variables adhere to a normal distribution with a constant variance-covariance matrix. Consequently, future interest rates also follow a normal distribution. This characteristic suggests that the ATSM might overestimate the probability of future interest rates turning negative in a low-interest-rate environment in which short-term interest rates are close to zero. As a result, time series analyses conducted in the low-interest-rate environment post the 2007–2008 global financial crisis have transitioned from using the ATSM to alternative models, such as the shadow rate model (SRM) or the quadratic Gaussian term structure model (QTSM). These models, unlike the ATSM, incorporate a lower bound on interest rates.

In the SRM, the short rate is defined as the higher value between a latent variable known as the shadow rate and a threshold that acts as a lower bound for interest rates. This model was first proposed by Black (1995) and later expanded upon by Gorovoi and Linetsky (2004). Empirical studies that use the SRM include those of Kim and Singleton (2012), Krippner (2013), Bauer and Rudebusch (2016), Wu and Xia (2016), Kortela (2016), Lemke and Vladu (2017), Ueno (2017), and Wu and Xia (2020). These studies analyze time series data from the United States, Europe, or Japan, and they encompass periods of quantitative easing. During these periods, a central bank buys financial assets from the financial market to increase liquidity and stimulate economic growth.

In the QTSM, as studied by Ahn et al. (2002) and Leippold and Wu (2002), the short rate is characterized as a quadratic function of the state variables. This model is unique in that a term structure of interest rates has a lower bound and their volatilities fluctuate stochastically based on the state variables. In empirical analyses, Nyholm and Vidova-Koleva (2012) estimate the QTSM using US yield curve data, and Kim and Singleton (2012) conduct similar estimations using Japanese yield curve data.

Empirical studies using the SRM and the QTSM have made significant contributions to the time series analysis of yield curves in low-interest rate environments, such as during the period of quantitative easing in the United States. However, except for the studies by Kortela (2016), Lemke and Vladu (2017), Ueno (2017), and Wu and Xia (2020), most of these studies use models with a constant lower bound on interest rates. This approach often misestimates the probability of future interest rate levels. For instance, when a large number of market participants anticipate a further deepening of the negative interest rate policy (NIRP), a model with a constant lower bound on interest rates would estimate the probability of future interest rates falling below a certain threshold as zero, potentially underestimating the actual probability.

To avoid misestimating the probabilities of future interest rate levels associated with changes in monetary policy stances, in particular, a deepening of NIRP, Wu and Xia (2020) develop an SRM based model. This model allows the lower bound of short-term interest rates to vary stochastically. In their model, two Markov chains representing the short- and long-term policy stances influence the lower bound on interest rates through the European Central Bank (ECB) deposit rate. They base their model on an approximate analytical solution for forward rates, which Wu and Xia (2016) previously derived. They then estimate their model using time series data from

the Euro Overnight Index Averages (EONIA) forward curves from July 2005 to June 2017. The estimation results fit the observed data well and show how the ECB's short- and long-term policy stances change.

This study adopts the idea proposed by Wu and Xia (2020) of making the lower bound on interest rates stochastic to capture changes in the probability distributions of future interest rates in response to monetary policy stances. Although their model focuses only on a deepening of NIRP without considering the exit from unconventional monetary policy (UMP), we incorporate the stochastic lower bound on interest rates varying with both a deepening of NIRP and the exit from the UMP. Our model extends the QTSM. Specifically, it characterizes the short rate as the sum of a positive interest rate component represented by a quadratic function of the state variables and a state variable driven by a Brownian bridge.¹ A model with only the first term would yield a QTSM with a zero lower bound. However, the second term brings a random lower bound for the interest rate. We assume that a Brownian bridge, which sets the lower bound on interest rates, is anchored at zero at two distinct time points. $t = 0$ denotes the date when negative interest rates were first observed, and $t = \tau$ denotes the effective end date of the UMP.² During the UMP period, market participants cannot predict precisely when the UMP will end. Therefore, our model treats τ as a random variable.³ The setting of this Brownian bridge has been studied in Bedini et al. (2017), and we use their results to derive the pricing of zero-coupon bonds under the no-arbitrage condition.

Our model proves effective in empirical analyses. We demonstrate this by estimating the model using time series data from the Japanese government bond (JGB) yield curve including negative interest rates. The results show that the model fits the observed data with high accuracy. Additionally, because our model is formulated in both risk-neutral and physical probability measures, it can handle risk premiums that reflect market expectations. As bond risk premiums, we calculate the expected JGB excess returns using estimates of model parameters and state variables to extract market expectations. The most significant feature of our model, which is not found in other term structure models, is its ability to calculate a probability distribution of the UMP's duration. Our empirical research uncovers shifts in market sentiments towards the UMP implemented by the Bank of Japan (BOJ) from October 2015 to June 2022 by

¹ Our modeling of the lower bound of interest rates is inspired by the work of Ajevskis and Vitola (2010). They use a Brownian bridge defined on $[0, r]$ to model the spread of short-term interest rates between the members of the European Monetary Union (EMU) and its candidate countries. The time r corresponds to when the candidate countries officially join the EMU, and their spreads converge to zero as the date approaches.

² The UMP might persist even after NIRP ends. As long as the UMP is in effect, market participants will anticipate the possibility of encountering negative interest rates again, even if the interest rates for all maturities momentarily exceed zero. Thus, in our research, we assume that the termination time τ of the Brownian bridge, which represents the lower bound on interest rates, corresponds to the last day of the UMP, not the last day of the NIRP.

³ This assumption is similar to that of Marumo et al. (2003), who assume that the short rate remains at zero until the end of a central bank's zero interest rate policy (ZIRP) and follows the Vasicek model once the ZIRP ends. They also treat the exit time from the ZIRP as a random variable and derive the bond pricing formula under the no-arbitrage condition.

calculating probability distributions for the duration of the UMP using estimates of model parameters and state variables.

The paper is organized as follows. Section 2 introduces the framework of our model. Sections 3 and 4 describe the derivations of the zero coupon bond pricing formulae for the cases where the end date of UMP is deterministic and random, respectively. Section 5 presents the estimation methodology, including the state space representation, parameter configuration, data set, and mathematical expressions for the expected excess bond returns and the posterior distribution of the UMP duration. Section 6 discusses the estimation results, and Section 7 concludes the paper.

2 Setup

We define a filtered probability space $(\Omega, \mathcal{F}, (\mathcal{F}_t)_{0 \leq t}, \mathbb{P})$ where the filtration $(\mathcal{F}_t)_{0 \leq t}$ satisfies the usual conditions of right-continuity and completeness and is the natural filtration generated by two stochastic processes X_t and y_t^τ as defined below. \mathbb{P} denotes the physical measure. $W_{t,x}^\mathbb{P} \in \mathbb{R}^n$ and $W_{t,y}^\mathbb{P} \in \mathbb{R}^1$ are independent standard Brownian motions under \mathbb{P} .

We assume that the market is complete and has no-arbitrage opportunities. This implies the existence of the unique risk-neutral measure \mathbb{Q} .

The state variable X_t satisfies the following stochastic differential equation under \mathbb{P} :

$$dX_t = K_X^\mathbb{P}(\theta^\mathbb{P} - X_t)dt + \Sigma_X dW_{t,x}^\mathbb{P}, \quad (1)$$

where all eigenvalues of the mean reversion coefficient matrix $K_X^\mathbb{P} \in \mathbb{R}^{n \times n}$ are assumed to be positive.

We assume that the risk-free short rate r_t is the sum of a quadratic function of X_t and y_t^τ :

$$r_t = X_t' \Psi X_t + y_t^\tau, \quad (2)$$

where X_t' represents the transposition of X_t and Ψ is positive-definite. Since $X_t' \Psi X_t > 0$, Eq. (2) implies that y_t^τ is the lower bound of r_t .

We define y_t^τ by the Brownian bridge process with $y_0^\tau = 0$, $y_\tau^\tau = 0$, and $y_t^\tau = 0$ for $t \geq \tau$. y_t^τ can be represented as

$$y_t^\tau = \sigma_y W_{t,y}^\mathbb{P} - \frac{\sigma_y t}{\tau \vee t} W_{\tau \vee t, y}^\mathbb{P}, \quad (3)$$

where $\tau \vee t = \max(\tau, t)$. Since $W_{t,x}^\mathbb{P}$ and $W_{t,y}^\mathbb{P}$ are independent as described above, y_t^τ is independent of X_t . For the time being, we assume that τ is a strictly positive constant value. Equation (3) is equivalent to the following Eq. (4) in the stochastic differential equation form:

$$dy_t^\tau = 1_{\{t \leq \tau\}} \left(-\frac{y_t^\tau}{\tau - t} dt + \sigma_y dW_{t,y}^{\mathbb{P}} \right). \tag{4}$$

Since Eq. (2) indicates that the short rate always becomes positive after time τ , interest rates at all maturities also become positive after time τ . Therefore, we can interpret τ as the date when the UMP ends.

The stochastic differential equation of X_t under \mathbb{Q} is assumed to be

$$dX_t = K_X^{\mathbb{Q}}(\theta^{\mathbb{Q}} - X_t)dt + \Sigma_X dW_{t,x}^{\mathbb{Q}}, \tag{5}$$

where $W_{t,x}^{\mathbb{Q}} \in \mathbb{R}^n$ is a standard Brownian motion under \mathbb{Q} , and $K_X^{\mathbb{Q}} \in \mathbb{R}^{n \times n}$ is a matrix with all eigenvalues being positive.

From Eqs. (1) and (5), we have the following relationship between $W_{t,x}^{\mathbb{Q}}$ and $W_{t,x}^{\mathbb{P}}$:

$$dW_{t,x}^{\mathbb{Q}} = dW_{t,x}^{\mathbb{P}} + \Lambda(X_t)dt, \tag{6}$$

where $\Lambda(X_t) = (K_X^{\mathbb{P}}\theta^{\mathbb{P}} - K_X^{\mathbb{Q}}\theta^{\mathbb{Q}}) - (K_X^{\mathbb{P}} - K_X^{\mathbb{Q}})X_t$. Here, $\Lambda(X_t)$ can be interpreted as the market price of factor risks. This affine form was first introduced in Duffee (2002) as the essentially affine market price of risk.

We incorporate the constant market price of risk, denoted as λ_y , associated with y_t^τ . This can be expressed as $dW_{t,y}^{\mathbb{Q}} = dW_{t,y}^{\mathbb{P}} + \lambda_y dt$. As a result, the dynamics of y_t^τ under the \mathbb{Q} measure is governed by the following equation:

$$dy_t^\tau = 1_{\{t \leq \tau\}} \left(-\frac{y_t^\tau}{\tau - t} dt - \sigma_y \lambda_y dt + \sigma_y dW_{t,y}^{\mathbb{Q}} \right). \tag{7}$$

As demonstrated in the Appendix, for $t \leq \tau$, the process y_t^τ follows a Brownian bridge with $y_0^\tau = 0$ and $y_\tau^\tau = 0$ under the \mathbb{Q} measure, and its probability density function $\phi_t^{\mathbb{Q}}(\tau, y_t^\tau)$ has the following representation:

$$\phi_t^{\mathbb{Q}}(\tau, y_t^\tau) = \sqrt{\frac{\tau}{2\pi t(\tau - t)\sigma_y^2}} \exp\left(-\frac{\tau(y_t^\tau - \sigma_y \lambda_y(\tau - t) \log \frac{\tau - t}{\tau})^2}{2t(\tau - t)\sigma_y^2}\right). \tag{8}$$

Setting $\lambda_y = 0$ in Eq. (8), we find that the probability density function $\phi_t^{\mathbb{P}}(\tau, y_t^\tau)$ of y_t^τ under \mathbb{P} has the following representation:

$$\phi_t^{\mathbb{P}}(\tau, y_t^\tau) = \sqrt{\frac{\tau}{2\pi t(\tau - t)\sigma_y^2}} \exp\left(-\frac{\tau y_t^{\tau 2}}{2t(\tau - t)\sigma_y^2}\right). \tag{9}$$

Remark 1 Although y_t^τ can be positive for $t < \tau$, y_t^τ is estimated to be negative if market yields are negative for at least one maturity. In simulating the path of y_t^τ based on the model, y_t^τ can be positive. This seems to cause a problem in that the probability that future interest rates will be positive becomes large, no matter if the

actual market participants believe that the UMP will persist. However, given that the posterior distribution of τ given in Eq. (39) is updated based on the value of y_t , the probability of τ arriving soon increases as y_t^τ approaches zero. This suggests that the above problem will not be significant.

3 Bond pricing in the case in which τ is deterministic

In this section, we derive a bond pricing formula in the case where τ is deterministic. We assume that τ is a strictly positive constant. From this point forward, we use a superscript of 'n' to represent a normal policy period, $\tau \leq t$ (the post-UMP period), and a superscript of 'unc' to denote a UMP period, $t < \tau$ (the UMP period).

3.1 Bond pricing in a normal policy period, post unconventional monetary policy period

In this subsection, we derive a zero coupon bond pricing formula in a normal policy period, $\tau \leq t$. This period corresponds to the post-UMP period.

An infinitesimal generator of X_t for $\tau \leq t$ is provided as

$$\mathcal{D}_t^n = (K_X^{\mathbb{Q}}(\theta^{\mathbb{Q}} - X_t))' \frac{\partial}{\partial X_t} + \frac{1}{2} \text{Tr} \left(\Sigma_X \Sigma_X' \frac{\partial^2}{\partial X_t \partial X_t'} \right). \quad (10)$$

Applying the Feynman–Kac theorem to the zero coupon bond price $P_{t,u}^n$ with maturity date $T = t + u$ leads to the following partial differential equation (PDE):

$$\left[\frac{\partial}{\partial t} + \mathcal{D}_t^n \right] P_{t,u}^n = r_t P_{t,u}^n, \quad P_{t,0}^n = 1. \quad (11)$$

We guess the solution form of Eq. (11) as follows:

$$P_{t,u}^n = \exp(X_t' A_u^n X_t + (b_u^n)' X_t + c_u^n). \quad (12)$$

Substituting Eq. (12) into Eq. (11), we obtain the following system of ordinary differential equations (ODEs) for A_u^n , b_u^n , and c_u^n :

$$\begin{aligned} \dot{A}_u^n &= -2K_X^{\mathbb{Q}'} A_u^n + 2A_u^n \Sigma_X \Sigma_X' A_u^n - \Psi, \\ (\dot{b}_u^n)' &= 2(K_X^{\mathbb{Q}} \theta^{\mathbb{Q}})' A_u^n - b_u^{n'} K_X^{\mathbb{Q}} + 2b_u^{n'} \Sigma_X \Sigma_X' A_u^n, \\ \dot{c}_u^n &= (K_X^{\mathbb{Q}} \theta^{\mathbb{Q}})' b_u^n + \text{Trace} \left(\Sigma_X \Sigma_X' \left(A_u^n + \frac{1}{2} b_u^n (b_u^n)' \right) \right), \end{aligned} \quad (13)$$

where \dot{A}_u^n , \dot{b}_u^n , and \dot{c}_u^n represent the derivatives of A_u^n , b_u^n , and c_u^n with respect to the variable u , and the boundary conditions are $A_0^n = 0$, $b_0^n = 0$, and $c_0^n = 0$, respectively.

3.2 Bond pricing under a UMP

In this subsection, we derive a zero coupon bond pricing formula in the case where $t < \tau$. This corresponds to the period when a central bank is conducting UMP.

First, we deal with the bond price with maturity date T that arrives before τ , the end date of the UMP. Denote the zero coupon bond price by $P_{t,u,w}^{unc,1}$, where $u = T - t$ and $w = \tau - T$. The price $P_{t,u,w}^{unc,1}$ is provided as follows:

$$\begin{aligned}
 P_{t,u,w}^{unc,1} &= E^{\mathbb{Q}} \left[\exp \left(- \int_t^T r_s ds \right) \middle| \mathcal{F}_t \right] \\
 &= E^{\mathbb{Q}} \left[\exp \left(- \int_t^T (X'_s \Psi X_s + y_s^\tau) ds \right) \middle| \mathcal{F}_t \right] \\
 &= E^{\mathbb{Q}} \left[\exp \left(- \int_t^T X'_s \Psi X_s ds \right) \middle| \mathcal{F}_t \right] E^{\mathbb{Q}} \left[\exp \left(- \int_t^T y_s^\tau ds \right) \middle| \mathcal{F}_t \right] \\
 &= P_{t,u}^n E^{\mathbb{Q}} \left[\exp \left(- \int_t^T y_s^\tau ds \right) \middle| \mathcal{F}_t \right],
 \end{aligned}
 \tag{14}$$

where $E^{\mathbb{Q}}[\cdot]$ is the expectation operator under \mathbb{Q} . The third equality in Eq. (14) holds by the independence between X_t and y_t^τ .

Since $P_{t,u}^n$ on the right-hand side of Eq. (14) is obtained from Eqs. (12) and (13), calculating the left-hand side of Eq. (14) reduces to calculating $P_{t,u,w}^y$ as follows:

$$P_{t,u,w}^y = E^{\mathbb{Q}} \left[\exp \left(- \int_t^T y_s^\tau ds \right) \middle| \mathcal{F}_t \right].
 \tag{15}$$

An infinitesimal generator of y_t^τ over $t < \tau$ for Eq. (7) is provided as

$$\begin{aligned}
 \mathcal{D}_t^{unc} &= - \frac{y_t^\tau}{\tau - t} \frac{\partial}{\partial y_t^\tau} - \sigma_y \lambda_y \frac{\partial}{\partial y_t^\tau} + \frac{1}{2} \sigma_y^2 \frac{\partial^2}{\partial y_t^2} \\
 &= - \frac{y_t^\tau}{u + w} \frac{\partial}{\partial y_t^\tau} - \sigma_y \lambda_y \frac{\partial}{\partial y_t^\tau} + \frac{1}{2} \sigma_y^2 \frac{\partial^2}{\partial y_t^2}.
 \end{aligned}
 \tag{16}$$

Applying the Feynman–Kac theorem to $P_{t,u,w}^y$ in Eq. (15), we obtain the following PDE:

$$\left[\frac{\partial}{\partial t} + \mathcal{D}_t^{unc} \right] P_{t,u,w}^y = y_t^\tau P_{t,u,w}^y, \quad P_{t,0,w}^y = 1.
 \tag{17}$$

We guess the solution of Eq. (17) as being in the following form:

$$P_{t,u,w}^y = \exp(d_{u,w}^{unc,1} y_t^\tau + f_{u,w}^{unc,1}).
 \tag{18}$$

Substituting Eq. (18) into Eq. (17), we obtain the following ODEs:

$$\begin{aligned} d_{u,w}^{unc,1} + \frac{d_{u,w}^{unc,1}}{u+w} + 1 &= 0, \\ f_{u,w}^{unc,1} &= \frac{1}{2}\sigma_y^2(d_{u,w}^{unc,1})^2 - \sigma_y\lambda_y d_{u,w}^{unc,1}, \end{aligned} \quad (19)$$

where the boundary conditions are $d_{0,w}^{unc,1} = 0$ and $f_{0,w}^{unc,1} = 0$, and $d_{u,w}^{unc,1}$ and $f_{u,w}^{unc,1}$ represent the derivatives of $d_{u,w}^{unc,1}$ and $f_{u,w}^{unc,1}$, respectively, with respect to the variable u . The first equation in Eq. (19) is known as d'Alembert's equation, and its solution is given as follows:

$$d_{u,w}^{unc,1} = -\frac{u(u+2w)}{2(u+w)}. \quad (20)$$

Equation (20) and the second equation in Eq. (19) lead to the solution of $f_{u,w}^{unc,1}$:

$$\begin{aligned} f_{u,w}^{unc,1} &= \int_0^u \left\{ \frac{1}{2}\sigma_y^2(d_{v,w}^{unc,1})^2 - \sigma_y\lambda_y d_{v,w}^{unc,1} \right\} dv \\ &= \frac{\sigma_y^2}{2} \int_0^u \frac{v^2(v+2w)^2}{4(v+w)^2} dv + \frac{\sigma_y\lambda_y}{2} \int_0^u \frac{v(v+2w)}{v+w} dv \\ &= \frac{\sigma_y^2}{24} \left((u+w)^3 - 6uw^2 + 2w^3 - \frac{3w^4}{u+w} \right) \\ &\quad + \frac{\sigma_y\lambda_y}{4} \left(u^2 + 2uw - 2w^2 \log \frac{u+w}{w} \right). \end{aligned} \quad (21)$$

Next, we derive the price representation of a zero coupon bond with a maturity date on or after the end date of the UMP, i.e., $t < \tau \leq T$. In this case, we denote the zero coupon bond price by $P_{t,u,w}^{unc,2}$, where $u = T - t$ and $w = \tau - T$. Then, $P_{t,u,w}^{unc,2}$ is given by:

$$\begin{aligned} P_{t,u,w}^{unc,2} &= E^{\mathbb{Q}} \left[\exp \left(- \int_t^T r_s ds \right) \middle| \mathcal{F}_t \right] = E^{\mathbb{Q}} \left[\exp \left(- \int_t^T (X'_s \Psi X_s + y_s^\tau) ds \right) \middle| \mathcal{F}_t \right] \\ &= E^{\mathbb{Q}} \left[\exp \left(- \int_t^T X'_s \Psi X_s ds \right) \middle| \mathcal{F}_t \right] E^{\mathbb{Q}} \left[\exp \left(- \int_t^T y_s^\tau ds \right) \middle| \mathcal{F}_t \right] \\ &= E^{\mathbb{Q}} \left[\exp \left(- \int_t^T X'_s \Psi X_s ds \right) \middle| \mathcal{F}_t \right] E^{\mathbb{Q}} \left[\exp \left(- \int_t^\tau y_s^\tau ds \right) \middle| \mathcal{F}_t \right] \\ &= P_{t,u}^n P_{t,u+w,0}^y. \end{aligned} \quad (22)$$

Note that $P_{t,u,w}^y = P_{t,u+w,0}^y$ when $w \leq 0$.

Thus, $P_{t,u+w,0}^y$ in Eq. (22) is calculated from Eqs. (18), (20), and (21) as follows:

$$\begin{aligned}
 P_{t,u+w,0}^y &= \exp(d_{u+w,0}^{unc,1} y_t^\tau + f_{u+w,0}^{unc,1}) \\
 &= \exp\left(-\frac{u+w}{2} y_t^\tau + \frac{\sigma_y^2}{24} (u+w)^3 + \frac{\lambda_y \sigma_y}{4} (u+w)^2\right). \tag{23}
 \end{aligned}$$

4 Bond pricing in the case in which τ is random

In this section, we derive a zero coupon bond pricing formula in the case where the end date of the UMP τ is random. Instead of Eq. (2), we define the risk-free short rate r_t as $r_t = X_t' \Psi X_t + y_t$. By this definition, y_t becomes the lower bound of interest rates. In this section, we model the lower bound of interest rates y_t as the Brownian bridge with the random interval length τ , which is studied in Bedini et al. (2017).

To price the zero coupon bonds, we need the probability distribution of τ under \mathbb{Q} . Thus, in this section, we focus on τ under \mathbb{Q} rather than \mathbb{P} . Let $\tau : \Omega \rightarrow (0, +\infty)$ be a strictly positive random variable with a distribution function denoted by $F(t) = \mathbb{Q}(\tau \leq t)$. We assume that τ is independent of $W_{t,x}^{\mathbb{Q}}$ and $W_{t,y}^{\mathbb{Q}}$. \mathcal{F}_t^y denotes the completed natural filtration generated by y_t ; that is, $\mathcal{F}_t^y = \sigma(y_s; 0 \leq s \leq t) \vee \mathcal{N}$, where \mathcal{N} denotes the collection of \mathbb{Q} -null sets. When we denote (C, \mathbf{C}) as the space of continuous real-valued functions on \mathbb{R}_+ endowed with the σ -algebra generated by the canonical process, we define a Brownian bridge with the random interval length τ as the map from (Ω, \mathcal{F}) to (C, \mathbf{C}) as follows:

Definition 1 The process $y_t(\omega)$ given by

$$y_t(\omega) = y_t^{\tau(\omega)}(\omega)$$

is the Brownian bridge with the random interval length $\tau(\omega)$, where y_t^r is the Brownian bridge defined in Eq. (3).

Bedini et al. (2017) prove that the mapping $y : (\Omega, \mathcal{F}) \rightarrow (C, \mathbf{C})$ is measurable, $\{y_t = 0\} = \{\tau \leq t\}$ for any $t > 0$, \mathbb{Q} -a.s., and the process y is a Markov process with respect to the natural filtration generated by y . We present their lemmas which are useful for deriving the zero coupon bond pricing formula in our setting below.

Lemma 2 Let $\sigma(\tau)$ denote the σ -algebra generated by τ and $\mathcal{B}(A)$ denote the Borel set of A .

If $h : ((0, +\infty) \times C, \mathcal{B}((0, +\infty)) \otimes \mathbf{C}) \rightarrow (\mathbb{R}, \mathcal{B}(\mathbb{R}))$ is a measurable function such that $E[|h(\tau, y)|] < +\infty$, then $E[h(\tau, y) | \sigma(\tau)](\omega) = E[h(r, y^r)]|_{r=\tau(\omega)}$, \mathbb{Q} -a.s.

Lemma 3 Let $0 \leq t \leq u$ and $g(\tau, y_u)$ be a $\sigma(y_s; s \geq t)$ measurable nonnegative function under \mathbb{Q} where $\sigma(y_s; s \geq t)$ is a sigma algebra generated by the future evolution of the process y . Then,

$$E^{\mathbb{Q}}[g(\tau, y_u) | \mathcal{F}_t^y] = E^{\mathbb{Q}}[g(\tau, y_u) | y_t], \mathbb{Q}\text{-a.s.}$$

Let $f^{\mathbb{Q}}(x)$ be the prior density function of τ under \mathbb{Q} . We define $G^{\mathbb{Q}}(t, y_t)$ as follows:

$$G^{\mathbb{Q}}(t, y_t) = \int_t^{\infty} \varphi_t^{\mathbb{Q}}(v, y_t) f^{\mathbb{Q}}(v) dv, \quad (24)$$

where $\varphi_t^{\mathbb{Q}}(r, y)$ is the density of y_t^r as in Eq. (8).

We present another lemma that was proved in Bedini et al. (2017) to use for the derivation of the zero coupon bond price representation:

Lemma 4 *Let $t > 0$ and $g(\tau, y_t)$ be a measurable function such that $g(\tau, y_t)$ is integrable. Then, \mathbb{Q} -a.s.*

$$E^{\mathbb{Q}}[g(\tau, y_t) | \mathcal{F}_t^y] = g(\tau, 0) 1_{\{\tau \leq t\}} + \int_t^{\infty} g(r, y_t) \frac{\varphi_t^{\mathbb{Q}}(r, y_t) f^{\mathbb{Q}}(r)}{G^{\mathbb{Q}}(t, y_t)} dr 1_{\{t < \tau\}}. \quad (25)$$

Note that Bayes' theorem implies that the expression $\frac{\varphi_t^{\mathbb{Q}}(r, y_t) f^{\mathbb{Q}}(r)}{G^{\mathbb{Q}}(t, y_t)}$ in Eq. (25) can be interpreted as the posterior density of τ conditioned on y_t .

We derive the pricing formula for the zero-coupon bond price $P_{t, T-t}$ with a maturity date of T at time t during a UMP period.

Proposition 5 *The following equation holds \mathbb{Q} -a.s.:*

$$\begin{aligned} 1_{\{t < \tau\}} P_{t, T-t} &= P_{t, T-t}^n E^{\mathbb{Q}} \left[\exp \left(- \int_t^T y_s ds \right) 1_{\{t < \tau\}} | \mathcal{F}_t^y \right] \\ &= \frac{1_{\{t < \tau\}}}{G^{\mathbb{Q}}(t, y_t)} \left(\int_T^{+\infty} P_{t, T-t, v-T}^{unc, 1} \varphi_t^{\mathbb{Q}}(v, y_t) f^{\mathbb{Q}}(v) dv + \int_t^T P_{t, T-t, v-T}^{unc, 2} \varphi_t^{\mathbb{Q}}(v, y_t) f^{\mathbb{Q}}(v) dv \right). \end{aligned}$$

Proof The first equality holds, owing to the independence between X_t and y_t . The term excluding $P_{t, T-t}^n$ on the right-hand side of the first equality is calculated \mathbb{Q} -a.s. as follows:

$$\begin{aligned} E^{\mathbb{Q}} \left[\exp \left(- \int_t^T y_s ds \right) 1_{\{t < \tau\}} | \mathcal{F}_t^y \right] &= E^{\mathbb{Q}} \left[\exp \left(- \int_t^T y_s ds \right) | y_t \right] 1_{\{t < \tau\}} \\ &= E^{\mathbb{Q}} \left[E^{\mathbb{Q}} \left[\exp \left(- \int_t^T y_s^r ds \right) | y_t^r \right]_{r=\tau} | y_t \right] 1_{\{t < \tau\}} \\ &= E^{\mathbb{Q}} \left[P_{t, T-t, \tau-T}^y(y_t^r) | y_t \right] 1_{\{t < \tau\}}. \end{aligned} \quad (26)$$

Since $\exp \left(- \int_t^T y_s ds \right) 1_{\{t < \tau\}}$ is a $\sigma(y_s; s \geq t)$ measurable nonnegative function, we obtain the first equality by applying Lemma 3. The second equality in Eq. (26) holds true due to Lemma 2. Third equality is given by Eqs. (15), (18), (22), and (23). Lemma

4 introduces the right-hand side of the final equality in the above equation into the following representation:

$$E^{\mathbb{Q}} \left[P_{t,T-t,\tau-T}^y(y_t) | y_t \right] 1_{\{t < \tau\}} = \frac{1}{G^{\mathbb{Q}}(t, y_t)} \left(\int_T^{+\infty} P_{t,T-t,v-T}^y \varphi_t^{\mathbb{Q}}(v, y_t) f^{\mathbb{Q}}(v) dv + \int_t^T P_{t,T-t,v-T}^y \varphi_t^{\mathbb{Q}}(v, y_t) f^{\mathbb{Q}}(v) dv \right) 1_{\{t < \tau\}}.$$

Thus, Eqs. (14), (22), and (26) lead to the conclusion of this proposition. □

We obtain the following pricing formula for $P_{t,T-t}$ by Proposition 5.

Theorem 6 *The following equation holds \mathbb{Q} -a.s.:*

$$P_{t,T-t} = P_{t,T-t}^n 1_{\{t \leq t\}} + \frac{1_{\{t < \tau\}}}{G^{\mathbb{Q}}(t, y_t)} \left(\int_T^{+\infty} P_{t,T-t,v-T}^{unc,1} \varphi_t^{\mathbb{Q}}(v, y_t) f^{\mathbb{Q}}(v) dv + \int_t^T P_{t,T-t,v-T}^{unc,2} \varphi_t^{\mathbb{Q}}(v, y_t) f^{\mathbb{Q}}(v) dv \right). \tag{27}$$

The first integrand on the right-hand side of Eq. (27) can be computed by applying the Gauss-Laguerre quadrature rule:

$$\int_T^{+\infty} P_{t,T-t,v-T}^{unc,1} \varphi_t^{\mathbb{Q}}(v, y_t) f^{\mathbb{Q}}(v) dv = \sum_{i=1}^n w_i^{GLa} P_{t,T-t,v_i^{GLa}}^{unc,1} \varphi_t^{\mathbb{Q}}(v_i^{GLa} + T, y_t) f^{\mathbb{Q}}(v_i^{GLa} + T) e^{v_i^{GLa}}, \tag{28}$$

where v_i^{GLa} and w_i^{GLa} are the nodes and weights of the Gauss-Laguerre quadrature, respectively.

The Gauss-Legendre quadrature rule is applied in the second integrand on the right-hand side of Eq. (27) as follows:

$$\int_t^T P_{t,T-t,v-T}^{a,2} \varphi_t^{\mathbb{Q}}(v, y_t) f^{\mathbb{Q}}(v) dv = \frac{T-t}{2} \sum_{i=1}^n w_i^{GLE} P_{t,T-t,v_i^{GLE-T}}^{a,2} \varphi_t^{\mathbb{Q}}(v_i^{GLE}, y_t) f^{\mathbb{Q}}(v_i^{GLE}), \tag{29}$$

where v_i^{GLE} and w_i^{GLE} are the nodes and weights of the Gauss-Legendre quadrature, respectively.

Equations (28) and (29) contribute to an efficient computation of bond prices.

5 Estimation methodology

In this section, we first present a state space representation of our proposed model. Next, we explain the assumptions we make for the model parameters and the historical data of the Japanese yield curve that we use to estimate the model. Additionally, we provide mathematical expressions for the expected excess bond returns and the posterior distributions of the UMP duration, which are plotted using the estimated state variables in the next section.

5.1 State space model representation

To estimate the latent factors X_t and y_t of our model, we apply a filtering method to a state space representation of the model. In this subsection, we formulate our model as a state space model.

The invariant transforms of Dai and Singleton (2000); Ahn et al. (2002), and Leipold and Wu (2002) are applicable to our model. This allows us to assume that $\theta^{\mathbb{P}}$ is a zero vector, Σ_X is the identity matrix, and $K_X^{\mathbb{P}}$ is the lower triangular matrix with positive diagonal elements. After applying the invariant transformation, we estimate the model.

The state equation of X_t describes the dynamics of X_t under the physical measure \mathbb{P} , as shown in Eq. (1). Replacing Eq. (1) with the discrete time representation under the time step Δt , we obtain the following equation:

$$X_{t+\Delta t} = \exp(-K_X^{\mathbb{P}} \Delta t) X_t + w_{X,t+\Delta t}, \quad (30)$$

where $w_{X,t+\Delta t} \sim N(0, V)$ and V is provided as follows:

$$(K_X^{\mathbb{P}} + (K_X^{\mathbb{P}})')^{-1} (I - \exp(-(K_X^{\mathbb{P}} + (K_X^{\mathbb{P}})') \Delta t)).$$

According to a theorem indicated in Bedini et al. (2017), y_t for $t < \tau$ satisfies the following equation:

$$\begin{aligned} y_t &= y_0 + \int_0^t E^{\mathbb{P}} \left[\frac{y_s}{\tau - s} \mid y_s \right] ds + \int_0^t \sigma_y dW_{s,y}^{\mathbb{P}} \\ &= y_0 - \int_0^t ds y_s \int_s^{\infty} dr \frac{\varphi_s^{\mathbb{P}}(r, y_s)}{(r - s) G^{\mathbb{P}}(s, y_s)} f^{\mathbb{P}}(r) 1_{\{s < \tau\}} + \int_0^t \sigma_y dW_{s,y}^{\mathbb{P}}, \end{aligned} \quad (31)$$

where $f^{\mathbb{P}}(\tau)$ is the prior density function for τ , the end time of the UMP under \mathbb{P} , $\varphi_t^{\mathbb{P}}(\tau, y_t)$ is the density function for y_t^{τ} under \mathbb{P} indicated in Eq. (9), and

$$G^{\mathbb{P}}(t, y_t) = \int_t^{\infty} \varphi_t^{\mathbb{P}}(v, y_t) f^{\mathbb{P}}(v) dv. \quad (32)$$

Let us denote $\int_s^\infty dr \frac{\varphi_s^{\mathbb{P}}(r, y_s)}{(r - s)G^{\mathbb{P}}(s, y_s)} f^{\mathbb{P}}(r)$ by $g(s)$. Then, Eq. (31) is rewritten in the following discrete time form:

$$y_{t+\Delta t} = e^{-\int_t^{t+\Delta t} g(s)ds} y_t + w_{y,t+\Delta t}, \tag{33}$$

where $w_{y,t+\Delta t} \sim N(0, V_y)$ and V_y is $\sigma_y^2 \int_t^{t+\Delta t} e^{-2\int_u^{t+\Delta t} g(s)ds} du$.

Let $Yield_t^{u_i}$ be the zero coupon yield with the time to maturity u_i at time t observed in a bond market. The vectors $Y_t^o = (Yield_t^{u_1}, \dots, Yield_t^{u_m})'$ and

$$Y_t(X_t, y_t) = \left(-\frac{1}{u_1} \log P_t^{u_1}(X_t, y_t), \dots, -\frac{1}{u_m} \log P_t^{u_m}(X_t, y_t) \right)'$$

computed from Eq. (27) constitute the observation equation of a state space model:

$$Y_t^o = Y_t(X_t, y_t) + \eta_t, \quad \eta_t \sim N(0, \eta^2 I_m), \tag{34}$$

where I_m is the identity matrix of size m . Errors η_t in the observation equation are assumed to follow a normal distribution with a zero mean vector and a diagonal covariance matrix $\eta^2 I_m$, and are assumed to be independent of other random variables.

Our state space model has a nonlinear observation equation; thus, we estimate the model parameters and latent factors X_t and y_t using the unscented Kalman filter (UKF) proposed by Julier and Uhlmann (1997). The extended Kalman filter (EKF) is a well-known filter that relies on the Taylor expansion of the nonlinear function. While the EKF is a derivative-based method, the UKF is a derivative-free method. Therefore, when it is difficult to differentiate the nonlinear function analytically, the UKF has an advantage over the EKF. In our case, because it is difficult to derive derivatives of the observation equations for y_t , we estimate the model parameters using the quasi-maximum likelihood method, while simultaneously estimating the latent variables X_t and y_t using the UKF.⁴

5.2 Parameter setting

We estimate the model using interest rates in the JGB market. To this end, this subsection presents the parameter settings.

Zero coupon interest rates with maturities of less than one year, estimated from JGB price data, often turned negative beginning in October 2015. Therefore, we establish the initial time of our model as September 30, 2015.

The duration of an event is frequently represented using an exponential distribution model. For instance, Ajevskis and Vitola (2010) presume that the time it takes for a country to become a member of the EMU follows an exponential distribution. A key characteristic of the exponential distribution is that the random variable generated

⁴ The UKF is used to estimate latent factors in some works in the finance literature (e.g., Leippold and Wu 2007; Christoffersen et al. 2014; Filipović et al. 2016; Branger et al. 2021).

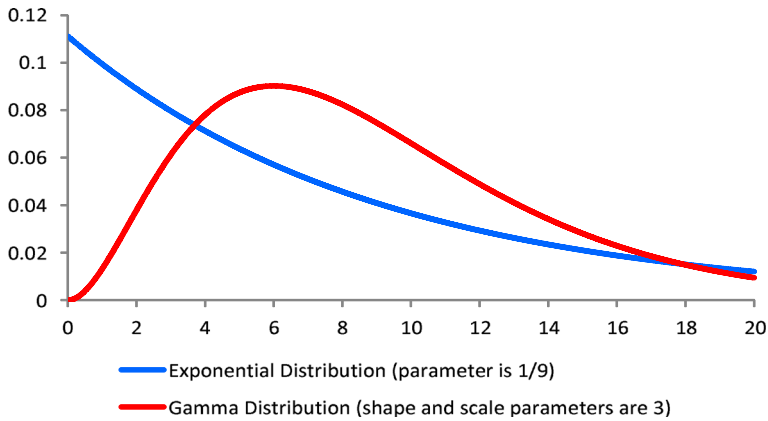


Fig. 1 Probability density functions of exponential distribution and gamma distribution

from the distribution is most likely to be zero, as depicted by the solid blue line in Fig. 1. However, this characteristic does not align with our findings, because numerous market participants believed the BOJ's UMP would persist when negative interest rates began to be observed.

Figure 1 shows the density function of a gamma distribution with the shape parameter $\alpha = 3$ and the scale parameter $\beta = 3$ in the solid red line. The density peaks at a point away from zero, and its expectation is $\alpha\beta$.

For this reason, we prefer a gamma distribution to an exponential distribution as the prior distribution of τ , denoted as $f^{\mathbb{P}}(\tau)$. We assume that the prior distribution of τ follows a gamma distribution with the shape parameter $\alpha = 3$ and the scale parameter $\beta = 3$, reflecting the expectations that the BOJ's UMP will continue for a prolonged period. Its density function is provided as follows:

$$f^{\mathbb{P}}(\tau) = \frac{\tau^{\alpha-1} e^{-\frac{1}{\beta}\tau}}{\beta^{\alpha} \Gamma(\alpha)} = \frac{\tau^2 e^{-\frac{1}{3}\tau}}{27\Gamma(3)}. \quad (35)$$

To maintain simplicity in estimation, we assume that $f^{\mathbb{Q}}(\tau) = f^{\mathbb{P}}(\tau)$ and that $K_X^{\mathbb{Q}}$ is the lower triangular matrix with positive diagonal elements as with $K_X^{\mathbb{P}}$.

Considering X_t as a three-dimensional latent state variable, we perform estimates under two conditions: (i) when the constraint $\lambda_y = 0$ is imposed, and (ii) when the constraint on λ_y is free.

5.3 Data

We estimate the model using market data for zero coupon yields of JGBs with maturities of 6 months, and 1, 2, 3, 5, 7, 10, and 20 years. The data spans from October 1, 2015, to June 8, 2022, with a frequency of every five business days starting from October 1, 2015. We estimate these yields based on B-spline regression, as detailed

Table 1 Summary statistics of bond yields: The data are JGB yields expressed as annual percentages

Maturity	Mean	Std. Dev	Skew	Kurt	Auto. Correl
0.5	-0.166	0.0852	-0.697	-0.139	0.962
1	-0.159	0.0729	-0.640	0.114	0.953
2	-0.147	0.0652	-0.207	0.898	0.931
3	-0.138	0.0685	-0.254	1.230	0.926
5	-0.126	0.0876	-0.608	0.905	0.939
7	-0.0864	0.106	-0.420	0.751	0.949
10	0.0423	0.119	-0.0867	0.932	0.964
20	0.532	0.213	0.901	1.841	0.982

Maturity is indicated in years. Mean is the sample mean, Std. Dev. is the standard deviation, Skew is the skewness, Kurt is the excess kurtosis, and Auto. Correl. is the first order autocorrelation

in Steeley (1991) and Kikuchi and Shintani (2012), using JGB prices from the Japan Securities Dealers Association.

Table 1 displays the summary statistics of the JGB yields used for our estimation. The results show that the mean term structure is upward sloping, the yields are negatively skewed, except for the 20-year rate, and the distributions of the medium and long-term rates exhibit thicker tails than the normal distribution.

5.4 Mathematical expressions for the expected excess bond returns and the posterior distribution of the duration of the UMP

Once all the parameters and state variables are estimated using the UKF and quasi-maximum likelihood methods, it is possible to compute suitable measures to shed light on the expectation formation of bond market participants. As examples, the following section presents estimates of the expected excess bond returns and the posterior distributions of the duration of the UMP (i.e., the time to exit the UMP). In preparation, this subsection offers mathematical expressions for the expected excess bond returns and the posterior distribution of the UMP duration.

First, we derive the expected excess return representation of the bond. Note that the sources of the expected excess returns in our model lie in X_t and y_t . Since X_t and y_t are independent, we consider the expected excess returns associated with X_t and y_t separately.

Regarding the expected excess returns attributable to X_t , the volatility matrix of a zero-coupon bond with a maturity date of T at time t with respect to the Brownian motion $W_{t,x}^{\mathbb{P}}$ is given by:

$$\frac{1}{P_{t,T-t}^n} \frac{\partial P_{t,T-t}^n}{\partial X_t'} \Sigma_X = ((A_{T-t}^n + (A_{T-t}^n)')X_t + b_{T-t}^n)' \Sigma_X.$$

This equation, along with Eq. (6), leads to the following representation of the excess return of bonds associated with X_t :

$$\left((A_{T-t}^n + (A_{T-t}^n)') X_t + b_{T-t}^n \right)' \Sigma_X \Lambda(X_t), \quad (36)$$

where $\Lambda(X_t)$ is defined in Eq. (6).

The excess returns attributable to y_t are given as follows:

$$\frac{1}{P_{t,T-t}} \frac{\partial P_{t,T-t}}{\partial y_t} \sigma_y \lambda_y. \quad (37)$$

Since $P_{t,T-t}$ is nonlinear in y_t as shown in Eq. (27), it is difficult to have an analytical derivative representation of $\frac{\partial P_{t,T-t}}{\partial y_t}$ in Eq. (37). Hence, we apply numerical differentiation for its computation in the following section.

The expected excess returns are obtained by taking the expected value under the physical probability measure in the sum of Eqs. (36) and (37). For computational simplicity, we use the filtered values $X_{t|t}$ for X in Eq. (36), and $y_{t|t}$ for y in Eq. (37). Thus, the expected excess bond return representation is given as follows:

$$\left((A_{T-t}^n + (A_{T-t}^n)') X_{t|t} + b_{T-t}^n \right)' \Sigma_X \Lambda(X_{t|t}) + \left(\frac{1}{P_{t,T-t}} \frac{\partial P_{t,T-t}}{\partial y_t} \right) \Big|_{y_t=y_{t|t}} \sigma_y \lambda_y. \quad (38)$$

The density function of the posterior distribution of τ under \mathbb{P} is expressed as:

$$\frac{\varphi_t^{\mathbb{P}}(\tau, y_t) f^{\mathbb{P}}(\tau)}{\int_t^{\infty} \varphi_t^{\mathbb{P}}(v, y_t) f^{\mathbb{P}}(v) dv}, \quad (39)$$

where $\varphi_t^{\mathbb{P}}(\tau, y_t)$ and $f^{\mathbb{P}}(\tau)$ are given in Eqs. (9) and (35), respectively.

Thus, at time $t < \tau$, Eq. (39) leads to the following density of the posterior distribution of the duration $s = \tau - t$ of UMP,

$$\frac{\varphi_t^{\mathbb{P}}(t + s, y_t) f^{\mathbb{P}}(t + s)}{\int_0^{\infty} \varphi_t^{\mathbb{P}}(t + s', y_t) f^{\mathbb{P}}(t + s') ds'}. \quad (40)$$

By denoting estimates of y_t by $y_{t|t}$, we can compute the posterior densities of the time to exit from the UMP under \mathbb{P} for each of the dates, using the estimates of the model parameters and $y_{t|t}$. From Eq. (40), these densities at time t are expressed as:

$$\frac{\varphi_t^{\mathbb{P}}(t + \tilde{\tau}, y_{t|t}) f^{\mathbb{P}}(t + \tilde{\tau})}{\int_0^{\infty} \varphi_t^{\mathbb{P}}(t + \tilde{\tau}, y_{t|t}) f^{\mathbb{P}}(t + \tilde{\tau}) d\tilde{\tau}}. \quad (41)$$

6 Estimation results

This section presents the results of our estimations. We perform estimates under two conditions: one with the constraint of $\lambda_y = 0$ and the other without it. We provide parameter estimates for both cases, and evaluate the fit using root mean square errors and comparisons between the observed and estimated values. Through these evaluations, we determine the better model and show estimates of its latent variable X_t and the lower bound of the interest rate y_t . These estimates, especially the estimates of y_t , provide insight into how the market perceived changes in the BOJ's stance on UMP. In addition, we present the expected excess returns of JGBs and the posterior probability distributions for the duration of the UMP based on the estimated values of X_t and y_t for the chosen model.

6.1 Parameter estimates and fitting

In this subsection, we perform the estimation under two cases: the case where the constraint $\lambda_y = 0$ is imposed, and the case where the constraint on λ_y is free. We call the former case “Case I” and the latter case “Case II”. As a benchmark to see how good both estimations are, we also show the estimation results in a model with a constant lower bound on the short rate (i.e. a model assuming $y_t^r = c$ in Eq. (2)). This is the “benchmark” model.

Table 2 presents the parameter estimation results for the benchmark and Cases I and II. The log-likelihood \mathcal{L} of the model with the constant lower bound (the benchmark model) is 17402 and its Bayesian information criterion (BIC) is -33779 , indicating that Cases I and II outperform the benchmark. Comparing Cases I and II, we find that the unconstrained case for λ_y (Case II) has larger log-likelihood values and a lower BIC than those of the $\lambda_y = 0$ case (Case I). Table 2 shows that the estimate of λ_y is statistically significant, confirming the validity of the model that incorporates λ_y .

Table 3 presents the root mean squared errors (RMSEs) for the estimated yields in the benchmark case, Case I, and Case II. The RMSEs of Cases I and II are smaller than those of the benchmark case. Notably, the RMSEs for all maturities in Cases I and II are consistently within two basis points in both cases, exhibiting strong in-sample performance.

Table 4 shows the descriptive statistics of the fitting errors for the benchmark case, Case I, and Case II. As shown, the maximum of the absolute values of the fitting errors in the benchmark case exceeds 10 basis points, whereas those of Cases I and II are at most around 7 basis points. Thus, Cases I and II exhibit good in-sample performance.

Tables 3 and 4 show that the estimation accuracy is equally good for Cases I and II. Given this and considering that Table 2 shows that the unconstrained case for λ_y has the lower BIC and the parameter estimate of λ_y is statistically significant, we henceforth focus on estimation results for the unconstrained case for λ_y .

Figures 2, 3, 4, and 5 compare the time series of observed and estimated yields of short-, medium-, and long-term interest rates, respectively, based on the model with the unconstrained case for λ_y . These figures demonstrate the high accuracy of our estimates.

Table 2 Parameter estimation results for the benchmark, Cases I, and II

Benchmark

$$\Psi = \begin{pmatrix} 3.9 \times 10^{-3} (0.0012) & -6.7 \times 10^{-4} (8.2 \times 10^{-5}) & -8.3 \times 10^{-5} (4.3 \times 10^{-5}) \\ -6.7 \times 10^{-4} (8.2 \times 10^{-5}) & 1.1 \times 10^{-4} (1.8 \times 10^{-5}) & 1.5 \times 10^{-5} (9.7 \times 10^{-6}) \\ -8.3 \times 10^{-5} (4.3 \times 10^{-5}) & 1.5 \times 10^{-5} (9.7 \times 10^{-6}) & 1.0 \times 10^{-4} (2.0 \times 10^{-5}) \end{pmatrix},$$

$$K_X^{\mathbb{P}} = \begin{pmatrix} 0.31 (0.20) & 0 & 0 \\ -1.2 (0.85) & 0.74 (0.49) & 0 \\ -0.57 (1.6) & -9.5 (2.2) & 5.5 (0.69) \end{pmatrix},$$

$$K_X^{\mathbb{Q}} = \begin{pmatrix} 9.6 (1.1) & 0 & 0 \\ 2.0 (1.1) & 0.0028 (0.0052) & 0 \\ -1.0 (2.2) & 0.29 (0.052) & 0.0024 (0.012) \end{pmatrix},$$

$$\theta^{\mathbb{Q}} = \begin{pmatrix} 1.3 (0.24) \\ 3.2 (0.40) \\ 9.3 (0.60) \end{pmatrix},$$

$$c = -0.0072 (2.3 \times 10^{-4}), \eta = 0.0245\%, \mathcal{L} = 17402.0, BIC = -33779$$

Case I

$$\Psi = \begin{pmatrix} 3.5 \times 10^{-8} (1.8 \times 10^{-8}) & -4.7 \times 10^{-9} (4.8 \times 10^{-9}) & -8.0 \times 10^{-9} (4.2 \times 10^{-9}) \\ -4.7 \times 10^{-9} (4.8 \times 10^{-9}) & 3.3 \times 10^{-5} (1.0 \times 10^{-5}) & 4.4 \times 10^{-5} (2.5 \times 10^{-5}) \\ -8.0 \times 10^{-9} (4.2 \times 10^{-9}) & 4.4 \times 10^{-5} (2.5 \times 10^{-5}) & 5.2 \times 10^{-4} (4.0 \times 10^{-5}) \end{pmatrix},$$

$$K_X^{\mathbb{P}} = \begin{pmatrix} 0.0075 (0.016) & 0 & 0 \\ 0.23 (0.13) & 1.3 \times 10^{-5} (1.5 \times 10^{-5}) & 0 \\ 0.027 (0.079) & -0.28 (0.64) & 3.2 \times 10^{-5} (1.3 \times 10^{-4}) \end{pmatrix},$$

$$K_X^{\mathbb{Q}} = \begin{pmatrix} 1.3 \times 10^{-9} (1.3 \times 10^{-9}) & 0 & 0 \\ -0.20 (0.0057) & 0.20 (0.037) & 0 \\ 0.041 (0.0060) & -0.26 (0.030) & 0.29 (0.059) \end{pmatrix},$$

$$\theta^{\mathbb{Q}} = \begin{pmatrix} 9.7 (0.26) \\ -1.0 (0.87) \\ 1.1 (0.37) \end{pmatrix},$$

$$\sigma_y = 0.0018 (2.0 \times 10^{-4}), \eta = 0.0126\%, \mathcal{L} = 18361.2, BIC = -36589$$

Case II

$$\Psi = \begin{pmatrix} 1.5 \times 10^{-5} (1.8 \times 10^{-6}) & -2.1 \times 10^{-5} (1.8 \times 10^{-6}) & 7.8 \times 10^{-6} (7.8 \times 10^{-7}) \\ -2.1 \times 10^{-5} (1.8 \times 10^{-6}) & 5.7 \times 10^{-5} (2.4 \times 10^{-7}) & 2.0 \times 10^{-5} (2.3 \times 10^{-6}) \\ 7.8 \times 10^{-6} (7.8 \times 10^{-7}) & 2.0 \times 10^{-5} (2.3 \times 10^{-6}) & 4.3 \times 10^{-4} (2.2 \times 10^{-6}) \end{pmatrix},$$

$$K_X^{\mathbb{P}} = \begin{pmatrix} 9.5 \times 10^{-4} (1.3 \times 10^{-3}) & 0 & 0 \\ 0.19 (0.012) & 0.0017 (0.0036) & 0 \\ -0.0081 (0.025) & -0.68 (0.0040) & 1.7 \times 10^{-4} (6.8 \times 10^{-5}) \end{pmatrix},$$

$$K_X^{\mathbb{Q}} = \begin{pmatrix} 4.1 \times 10^{-7} (1.3 \times 10^{-7}) & 0 & 0 \\ -0.18 (4.9 \times 10^{-5}) & 0.20 (8.2 \times 10^{-4}) & 0 \\ 0.028 (5.2 \times 10^{-4}) & -0.31 (0.0022) & 0.30 (0.0031) \end{pmatrix},$$

$$\theta^{\mathbb{Q}} = \begin{pmatrix} 9.8 (0.0012) \\ -1.6 (0.015) \\ 1.3 (0.082) \end{pmatrix},$$

$$\sigma_y = 0.0019 (6.2 \times 10^{-5}), \lambda_y = 0.25 (0.0083),$$

$$\eta = 0.0124\%, \mathcal{L} = 18422.8, BIC = -36707$$

The standard errors are indicated in parentheses. η is defined as Eq. (34); \mathcal{L} is the optimal log-likelihood; and BIC is the Bayesian information criterion

Table 3 The root mean squared errors (RMSE) for estimated yields are reported in basis points with maturity indicated in years

Maturity	0.5	1	2	3	5	7	10	20
Benchmark	1.54	1.59	1.93	1.70	2.24	2.83	3.16	2.42
Case I	1.16	0.714	0.860	0.953	1.05	1.54	1.41	0.858
Case II	1.08	0.626	0.842	0.950	0.993	1.48	1.31	1.01

“Benchmark” in the table corresponds to the model with a constant lower bound. “Case I” and “Case II” correspond to the $\lambda_\gamma = 0$ case and the unconstrained case for λ_γ , respectively

Table 4 Fitting errors are reported in basis points with maturity indicated in years

Maturity	0.5	1	2	3	5	7	10	20
<i>Benchmark</i>								
Mean	-0.167	0.819	1.130	0.665	-1.530	-1.958	2.147	-0.300
Std	1.530	1.368	1.564	1.565	1.635	2.046	2.314	2.404
Min	-5.014	-4.555	-3.462	-4.523	-9.516	-9.554	-4.303	-10.725
25%	-0.930	0.241	0.160	-0.254	-2.287	-3.301	0.412	-1.565
50%	-0.346	1.144	0.965	0.601	-1.450	-1.739	1.995	-0.254
75%	0.474	1.638	2.092	1.650	-0.650	-0.762	3.910	0.704
Max	10.306	4.925	6.643	8.859	5.228	4.733	9.930	10.010
<i>Case I</i>								
Mean	0.338	-0.230	-0.106	0.429	0.116	-0.503	0.264	-0.0150
Std	1.108	0.676	0.853	0.851	1.048	1.455	1.388	0.857
Min	-5.456	-4.619	-3.102	-1.946	-5.220	-6.471	-4.614	-6.107
25%	-0.172	-0.393	-0.742	-0.207	-0.558	-1.445	-0.864	-0.316
50%	0.329	-0.148	-0.142	0.429	0.111	-0.504	0.320	0.0822
75%	0.860	0.0419	0.523	0.989	0.878	0.476	1.111	0.383
Max	5.306	2.362	3.670	3.823	3.014	3.465	7.126	3.364
<i>Case II</i>								
Mean	0.401	-0.198	-0.0755	0.447	0.111	-0.510	0.278	-0.0249
Std	1.005	0.594	0.838	0.838	0.987	1.391	1.275	1.007
Min	-3.531	-3.202	-2.772	-1.626	-3.346	-5.215	-3.284	-6.990
25%	-0.193	-0.397	-0.721	-0.219	-0.531	-1.422	-0.804	-0.409
50%	0.328	-0.164	-0.093	0.487	0.104	-0.600	0.360	0.0756
75%	0.906	0.0324	0.530	1.022	0.891	0.486	1.094	0.429
Max	4.273	2.270	3.425	3.539	2.603	3.668	6.413	3.682

The mean represents the sample average of fitting errors, the standard deviation is denoted by Std, and the minimum and maximum values are denoted by Min and Max, respectively. The fitting errors' quartiles are presented as 25%, 50%, and 75%

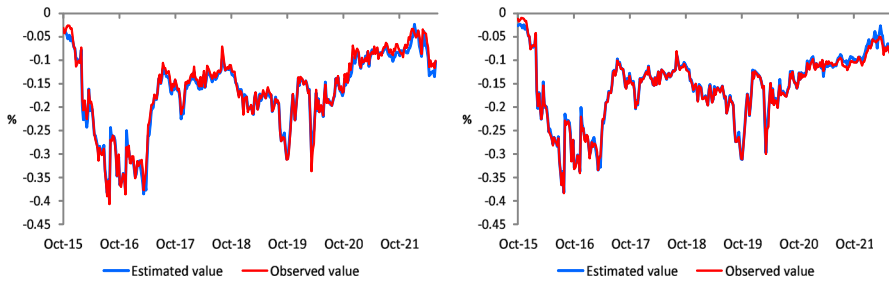


Fig. 2 Comparison between observed and estimated values of 6-month and 1-year yields

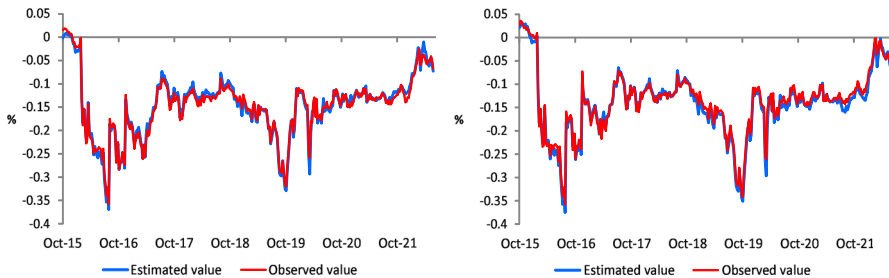


Fig. 3 Comparison between observed and estimated values of 2-year and 3-year yields

6.2 State variable estimates

Our model has two state variables, X_t and y_t . Since these variables are unobservable, in this subsection, we estimate them using the unscented Kalman filter.

Figure 6 shows the filtered value of X , or $X_{t|t}$. In the following subsection, we plot the evolution of the expected excess bond returns with different maturities using this filtered value, $X_{t|t}$ and $y_{t|t}$ shown thereafter.

Figure 7 displays the estimated values of the stochastic lower bound, y . As shown in Fig. 7, y shows a significant decrease during the summers of 2016 and 2019. The first decrease can be attributed to the growing belief that the BOJ would deepen its NIRP during this period. Similarly, the second decrease is attributed to the BOJ's forward guidance on the policy rate at the Monetary Policy Meeting held in April 2019. The Bank's decision to clarify its forward guidance on the policy rate and to take some policy actions to continue its strong monetary easing, as discussed in Bank of Japan Financial Markets Department (2020), likely drove the decrease in 2019.

6.3 Expected excess bond returns

Once we obtain estimates of the state variables X_t and y_t , we can compute informative indicators to clarify the expectation formation of bond market participants. As an example of such indicators, this subsection shows the expected excess returns on JGBs using the estimates of the model parameters and state variables in Sects. 6.1 and 6.2, respectively. The computation is implemented using Eq. (38).

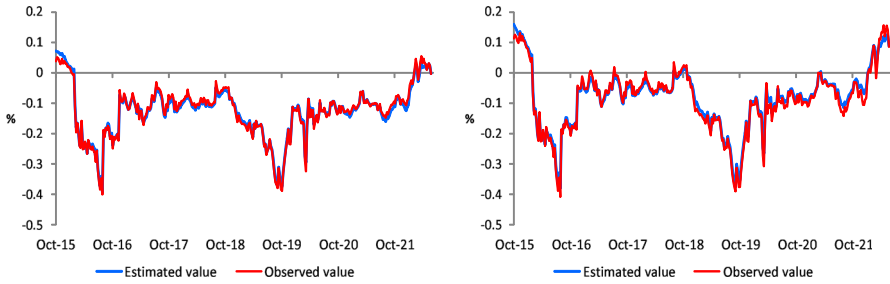


Fig. 4 Comparison between observed and estimated values of 5-year and 7-year yields

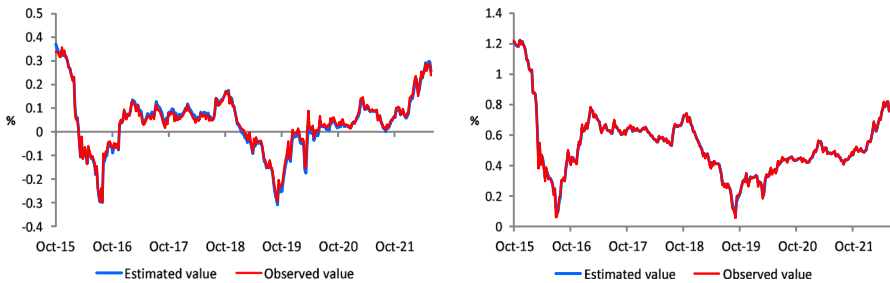


Fig. 5 Comparison between observed and estimated values of 10-year and 20-year yields

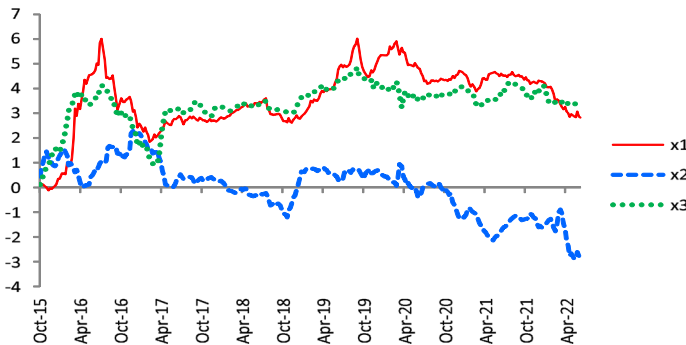


Fig. 6 Estimates of X_t , denoted as $X_{t|t}$, with its components labeled x_1 , x_2 , and x_3

Figure 8 shows the expected excess returns for bonds with maturities of one, two, five, ten, and twenty years. The figure reveals that the expected excess returns for all bond maturities remain consistently low throughout the sample period, with negative values for much of the time. The figure also shows a deeper plunge into negative territory for expected excess bond returns in 2016 and 2019, possibly indicating the market’s belief that the BOJ was leaning toward further monetary easing. Additionally, the expected excess return for short-term bonds becomes positive in 2021, followed by a positive turn for long-term bonds in 2022. This shift could reflect the BOJ’s decision to expand the target range for the 10-year JGB rate under the yield curve control (YCC) policy at the March 2021 monetary policy meeting.

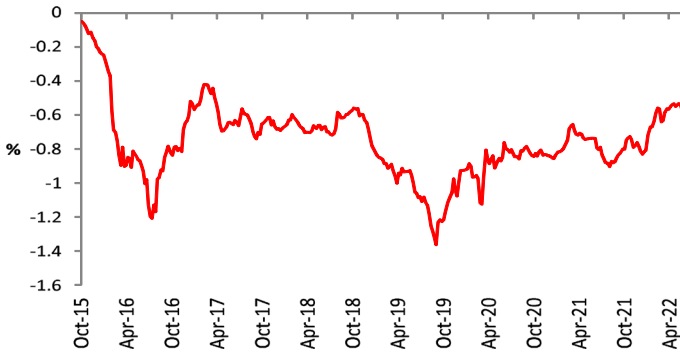


Fig. 7 Estimates of the stochastic lower bound y_t , or $y_t|t$

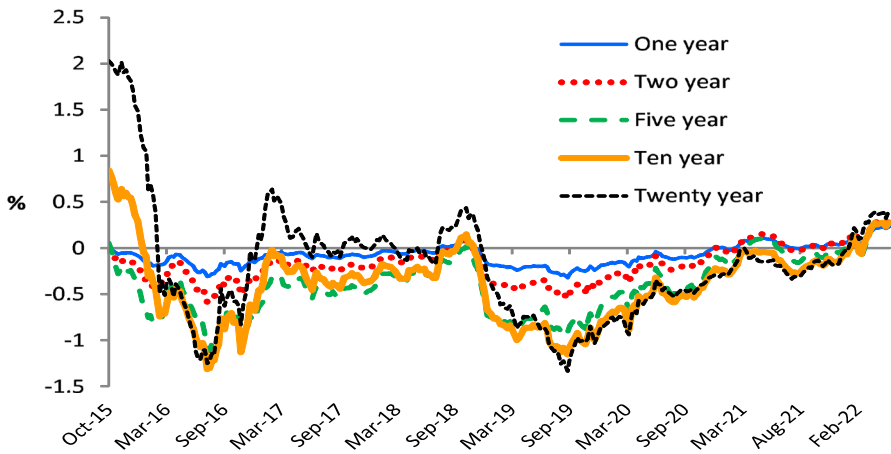


Fig. 8 Expected excess bond returns

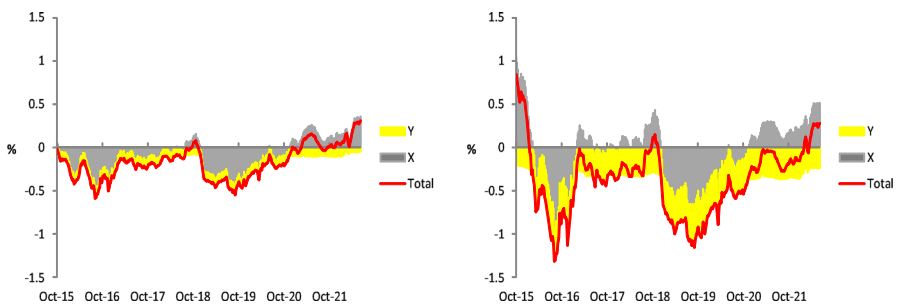


Fig. 9 Factor decomposition of the expected excess returns of two-year bond (left figure) and 10-year bond (right figure). In the figure, the gray portion represents the expected excess return attributed to X , and the yellow portion indicates the expected excess return attributed to y

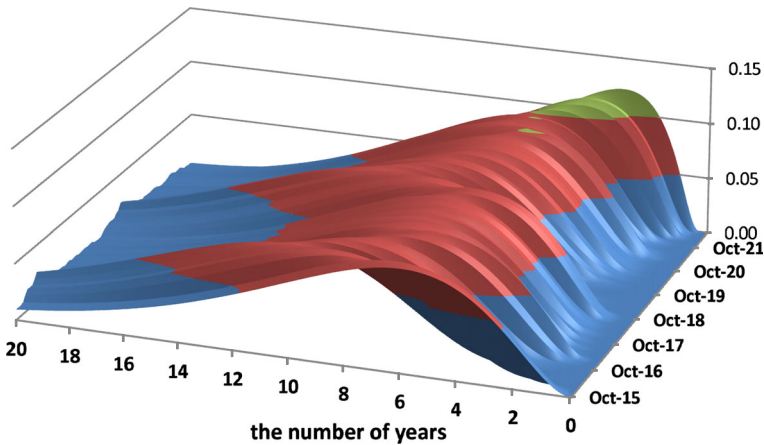


Fig. 10 Changes in the distribution of UMP duration over time

In our model, expected excess returns can be decomposed into factors associated with X_t and y_t based on Eqs. (36) and (37), respectively. Figure 9 shows the decomposition of expected excess returns on two-year and 10-year bonds into factors attributable to X_t and y_t . The figure shows that the contribution of y_t puts downward pressure on the expected excess returns for both bonds. We also find that the relative contribution of y_t to the total is more outstanding for the 10-year bond than it is for the two-year bond throughout the period.

6.4 Implied posterior distribution of the UMP duration

Market participants show a strong interest in when a UMP will end. To examine this, we present how market participants' perceptions of the duration of UMP have changed over time, based on the posterior distributions of the duration of UMP provided in Eq. (41).

Figure 10 shows the changes in the posterior distribution of the duration of the UMP over time, which we compute by substituting the estimates of the model parameters and state variables in Sects. 6.1 and 6.2 into Eq. (41), respectively. The figure shows that the posterior distribution of the UMP duration shifts toward shorter durations as the sample period approaches its end.

We compute the expected values and modes of the UMP duration from the distributions in Fig. 10, and plot them in Fig. 11. The figure shows that, compared with Fig. 7, the expected values and modes exhibit a reversal and a decreasing trend from the end of September 2019. In particular, the decrease is significant and pronounced from the beginning of 2022.

Figure 12 shows a comparison of the implied posterior distributions for the duration of the UMP on four selected days from the sample. The BOJ introduced NIRP in January 2016, and by the middle of that year, there was increasing market speculation that the policy would be intensified. This speculation might have caused the peak of

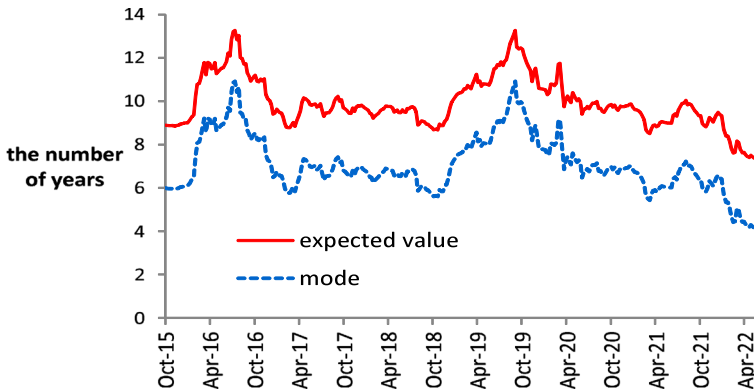


Fig. 11 Estimated values and modes computed from implied posterior distributions of UMP duration

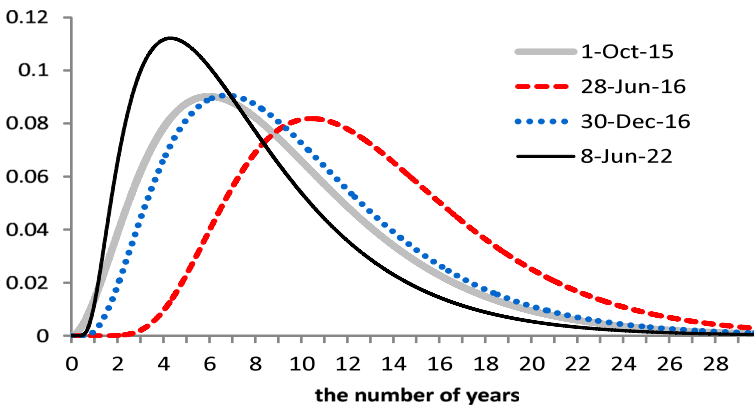


Fig. 12 Implied posterior distributions of UMP duration

the distribution in Fig. 12 on June 28, 2016, to shift to the right compared with its position on October 2015. However, the BOJ did not intensify the NIRP. Instead, it introduced the YCC policy in September 2016. Figure 12 indicates that this action by the BOJ resulted in shorter forecasts for the duration of the UMP. In early 2022, the market became more conscious of the potential for a YCC revision by the BOJ, causing the implied distribution in June 2022 to shift leftward compared with other distributions. By 2023, the market's interest in the possibility of the BOJ revising the YCC had become even more noticeable. Therefore, if we extend the sample period to 2023 and estimate the model, the resulting posterior probability distribution might differ from the one obtained in 2022.

7 Conclusion

This paper has presented a novel model of the term structure of interest rates to analyze time series data of yield curves, including the period of negative interest rate policy

in the sample. The model defines the short rate as the sum of a quadratic function of Gaussian state variables and a stochastic lower bound on interest rates modeled by a Brownian bridge anchored at zero at time zero and at a random positive time. The former time represents the first appearance of negative interest rates in the market and the latter time represents the end of a UMP. The inclusion of such a Brownian bridge lower bound is intended to allow the term structure model to capture changes in the actual yield curves associated with both the strengthening and loosening of the UMP. Within this framework, we have derived a semi-analytical pricing formula for zero coupon bonds under the no-arbitrage condition.

In an empirical study, we have used time series data on the Japanese yield curve to estimate the state variables and parameters, thereby demonstrating the effectiveness of our proposed model. The model aligns well with the data, as evidenced by the small RMSEs between the estimated and observed yield curves. Furthermore, our estimates reveal a significant drop in the lower bound of the interest rate during the middle of 2016 and around September 2019. This finding aligns with the speculation about the deepening of the NIRP that prevailed in the financial market in 2016. It is also consistent with the growing market expectations in September 2019 that the BOJ would take further monetary easing.

After estimating the parameters and state variables of the model, we calculated the expected excess returns of JGBs across various maturities, which serve as indicators of interest in the financial market. Our findings reveal that the expected excess returns of JGBs remain consistently low throughout the sample period, even becoming negative for much of the time. This trend is largely due to the BOJ's ongoing large-scale monetary easing policy. Additionally, we calculated the posterior probability distributions for the duration of the UMP based on the estimated parameters and state variables. This helps to show how financial market participants form their expectations for the UMP. Our findings indicate that participants anticipated a longer duration of the UMP in the middle of 2016 and September 2019. They also show that expectations for the duration decreased rapidly from the beginning of 2022.

While we have demonstrated the application of our proposed model using time series data of the Japanese yield curve, it could also be applied to analyze the yield curves of European countries that have experienced negative interest rates. Although Europe returned to positive interest rates in 2022, it had experienced negative interest rates in the past. Therefore, it would be worthwhile for future research to investigate how the model performs using time series data that includes both negative and positive interest rate periods in Europe.

Acknowledgements The author gratefully acknowledges the valuable comments provided by the editor and the anonymous referee.

Funding This work was supported by JSPS KAKENHI Grant Number (C) JP17K03802, JP20K01768 and by a Grant-in-Aid from Zengin Foundation for Studies on Economics and Finance.

Declarations

Conflict of interest The author declares that he has no conflict of interest.

Ethical approval The author's study does not involve either human or animal participants.

Appendix

A proof that y_t^τ is the Brownian bridge with $y_0^\tau = 0$ and $y_\tau^\tau = 0$ under \mathbb{Q} and its density follows Eq. (8) for $t \leq \tau$.

We first compute the Ito derivative of $\frac{y_t^\tau}{\tau - t}$ as follows:

$$\begin{aligned} d\left(\frac{y_t^\tau}{\tau - t}\right) &= \frac{dy_t^\tau}{\tau - t} + \frac{y_t^\tau dt}{(\tau - t)^2} = -\frac{y_t^\tau}{(\tau - t)^2}dt - \frac{\sigma_y \lambda_y}{\tau - t}dt + \frac{\sigma_y dW_{t,y}^\mathbb{Q}}{\tau - t} + \frac{y_t^\tau dt}{(\tau - t)^2} \\ &= -\frac{\sigma_y \lambda_y}{\tau - t}dt + \frac{\sigma_y dW_{t,y}^\mathbb{Q}}{\tau - t}. \end{aligned}$$

The second equality holds from Eq. (7).

Integrating both sides of the above equation from 0 to t , we obtain the following equation:

$$\begin{aligned} \int_0^t d\left(\frac{y_s^\tau}{\tau - s}\right) &= \frac{y_t^\tau}{\tau - t} - \frac{y_0^\tau}{\tau} = -\int_0^t \frac{\sigma_y \lambda_y}{\tau - s} ds + \int_0^t \frac{\sigma_y dW_{s,y}^\mathbb{Q}}{\tau - s} \\ &= \sigma_y \lambda_y \log \frac{\tau - t}{\tau} + \int_0^t \frac{\sigma_y dW_{s,y}^\mathbb{Q}}{\tau - s}. \end{aligned}$$

Since $y_0^\tau = 0$, we have

$$y_t^\tau = \sigma_y \lambda_y (\tau - t) \log \frac{\tau - t}{\tau} + \sigma_y (\tau - t) \int_0^t \frac{dW_{s,y}^\mathbb{Q}}{\tau - s}.$$

Hence, y_t^τ follows a normal distribution with the expectation

$$E^\mathbb{Q}[y_t^\tau] = \sigma_y \lambda_y (\tau - t) \log \frac{\tau - t}{\tau}$$

and the variance

$$Var^\mathbb{Q}[y_t^\tau] = \sigma_y^2 (\tau - t)^2 \int_0^t \frac{ds}{(\tau - s)^2} = \frac{\sigma_y^2 t (\tau - t)}{\tau}.$$

This means that Eq. (8) holds.

Since $\lim_{t \rightarrow \tau} (\tau - t) \log(\tau - t) = 0$, $\lim_{t \rightarrow \tau} y_t^\tau = 0$. Therefore, y_t^τ is the Brownian bridge with $y_0^\tau = 0$ and $y_\tau^\tau = 0$ under \mathbb{Q} .

References

- Ahn, D.-H., Dittmar, R.F., Gallant, A.R.: Quadratic term structure models: theory and evidence. *Rev. Financ. Stud.* **15**(1), 243–288 (2002)
- Ajevsksis, V., Vitola, K.: A convergence model of the term structure of interest rates. *Rev. Financ.* **14**(4), 727–747 (2010)
- Ang, A., Piazzesi, M.: A no-arbitrage vector autoregression of term structure dynamics with macroeconomic and latent variables. *J. Monet. Econ.* **50**(4), 745–787 (2003)
- Bank of Japan Financial Markets Department.: Market Operations in Fiscal 2019. Bank of Japan (2020)
- Bauer, M.D., Rudebusch, G.D.: Monetary policy expectations at the zero lower bound. *J. Money Credit Bank* **48**(7), 1439–1465 (2016)
- Bedini, M.L., Buckdahn, R., Engelbert, H.-J.: Brownian bridges on random intervals. *Theor. Probab. Appl.* **61**(1), 15–39 (2017)
- Black, F.: Interest rates as options. *J. Financ.* **50**(5), 1371–1376 (1995)
- Branger, N., Herold, M., Muck, M.: International stochastic discount factors and covariance risk. *J. Bank Financ.* **123**, 1 (2021)
- Christoffersen, P., Dorion, C., Jacobs, K., Karoui, L.: Nonlinear Kalman filtering in affine term structure models. *Manag. Sci.* **60**(9), 2248–2268 (2014)
- Dai, Q., Singleton, K.J.: Specification analysis of affine term structure models. *J. Financ.* **55**(5), 1943–1978 (2000)
- Duffee, G.R.: Term premia and interest rate forecasts in affine models. *J. Financ.* **57**(1), 405–443 (2002)
- Filipović, D., Gourier, E., Mancini, L.: Quadratic variance swap models. *J. Financ. Econ.* **119**(1), 44–68 (2016)
- GOROVOI, V., LINETSKY, V.: Black’s model of interest rates as options, Eigenfunction expansions and Japanese interest rates. *Math. Financ.* **14**(1), 49–78 (2004)
- Julier, S.J., Uhlmann, J.K.: A new extension of the Kalman filter to nonlinear systems. *Proc SPIE Conf on Sign Proces, Sensor Fusion, and Target Recognition VI.* **3068**, 182–193 (1997)
- Kikuchi, K., Shintani, K.: Comparative analysis of zero coupon yield curve estimation methods using JGB price data. *Monet. Econ. Stud.* **30**, 75–122 (2012)
- Kim, D.H., Orphanides, A.: Term structure estimation with survey data on interest rate forecasts. *J. Financ. Quant. Anal.* **47**(1), 241–272 (2012)
- Kim, D.H., Singleton, K.J.: Term structure models and the zero bound: an empirical investigation of Japanese yields. *J. Econom.* **170**(1), 32–49 (2012)
- Kortela, T.: A shadow rate model with time-varying lower bound of interest rates. Bank of Finland Research Discussion Paper No.19, Bank of Finland (2016)
- Krippner, L.: Measuring the stance of monetary policy in zero lower bound environments. *Econ. Lett.* **118**(1), 135–138 (2013)
- Leippold, M., Wu, L.: Asset pricing under the quadratic class. *J. Financ. Quant. Anal.* **37**(2), 271–295 (2002)
- Leippold, M., Wu, L.: Design and estimation of multi-currency quadratic models. *Rev. Financ.* **11**(2), 167–207 (2007)
- Lemke, W., Vladu, A.L.: Below the zero lower bound: a shadow-rate term structure model for the Euro area. Working Paper No.1991. European Central Bank (2017)
- Marumo, K., Nakayama, T., Nishioka, S., Yoshida, T.: Extracting market expectations on the duration of the zero interest rate policy from Japan’s bond prices. Financial Markets Department Working Paper 03-E-2. Bank of Japan (2003)
- Nyholm, K., Vidova-Koleva, R.: Nelson-Siegel affine and quadratic yield curve specifications: which one is better at forecasting? *J. Forecast.* **31**(6), 540–564 (2012)
- Steeley, J.M.: Estimating the gilt-edged term structure: basis splines and confidence intervals. *J. Bus. Financ. Account.* **18**(4), 513–529 (1991)
- Ueno, Y.: Term structure models with negative interest rates. IMES Discussion Paper Series 17-E01, Institute for Monetary and Economic Studies, Bank of Japan (2017)

- Wu, J.C., Xia, F.D.: Measuring the macroeconomic impact of monetary policy at the zero lower bound. *J. Money Credit Bank* **48**(2–3), 253–291 (2016)
- Wu, J.C., Xia, F.D.: Negative interest rate policy and yield curve. *J. Appl. Econom.* **35**(6), 653–672 (2020)

Publisher's Note Springer Nature remains neutral with regard to jurisdictional claims in published maps and institutional affiliations.

Springer Nature or its licensor (e.g. a society or other partner) holds exclusive rights to this article under a publishing agreement with the author(s) or other rightsholder(s); author self-archiving of the accepted manuscript version of this article is solely governed by the terms of such publishing agreement and applicable law.